Analysis of flow resistance property for valve-less piezoelectric pump with hemisphere-segment bluff-body

Shengduo Li[1], Wei Zhao[1], Jing Ji[1*], Caiqi Hu[1*], Xiaoqi Hu[2]

(1. *College of Mechanical and Electrical Engineering, Qingdao Agricultural University, Qingdao 266109, China*;
2. *College of Mechanical and Electrical Engineering, Zaozhuang University, Zaozhuang 277160, China*)

Abstract: Based on the principle that the flow resistances on spherical surface and round surface of hemisphere-segment in pump chamber are unequal, a novel valve-less piezoelectric pump with hemisphere-segment bluff-body (HSBB) is presented. The pumping performance depends directly on the flow resistances and their change law on hemisphere-segment surfaces. Therefore, it is necessary to study the flow resistance property of HSBB. This study finds that the forward and reverse flow resistances on HSBB cannot be solved simultaneously by traditional theoretical and experimental hydrodynamics equivalent method for flow resistance around non-sphere. Based on the geometric features of hemisphere-segment the method of Equivalent Flow Resistance Diameter was proposed, and the forward and reverse equivalent spheres respectively corresponding to the spherical and round surface of hemisphere-segment were separated and the sphere diameters were calculated. Flow resistance measuring device was designed, and the flow resistance coefficient of hemisphere-segment was obtained by testing and calculating. The theoretical formulas of forward and reverse flow resistance on hemisphere-segment were established. And through experiments it is verified that the method proposed in this paper is feasible and can be applied to analyze and calculate flow resistance and pumping flow rate in pump.

Keywords: valve-less piezoelectric pump, equivalent flow resistance, flow around hemisphere-segment, flow resistance coefficient

DOI: 10.33440/j.ijpaa.20210401.149

Citation: Li S D, Zhao W, Ji J, Hu C Q, Hu X Q. Analysis of flow resistance property for valve-less piezoelectric pump with hemisphere-segment bluff-body. Int J Precis Agric Aviat, 2021; 4(1): 14–21.

1 Introduction

Based on the converse piezoelectric effect of the piezoelectric ceramics, valve-less piezoelectric pump is a new type of fluid machine, which has no-moving part as valve in the chamber. Valve-less piezoelectric pumps utilize the deformation of piezoelectric vibrator to change the pump chamber volume so as to pump fluid. Because of no-moving part in pump chamber, the service life and reliability of the pump can be guaranteed. And the simple structure of the pump is beneficial to Micro Electro Mechanical Systems (MEMS) processing. Valve-less piezoelectric pump has great potential on application in biology, medical treatment[1] , chemical industry[2], and fuel supplement by micro mechanism[3]. At present, there are two kinds of pumps on UAV (unmanned aerial vehicle)[4-6]: diaphragm pump and peristaltic pump. Both of them and valveless pump (valveless piezoelectric pump) are all volumetric pumps. Compared with diaphragm pump and peristaltic pump, valveless pump has the following advantages: no independent driving source, no noise, no diaphragm or hose wear; small size, light weight, easy integration; and good flow regulation, due to the introduction of the hemisphere-segment as a bluff-body "valve", so the liquid pumping at the same time can achieve the mixed function of the liquid, such as water, fertilizer, pesticide and other mixed pumping. It has significant advantages in precision agriculture and plant protection spraying.

There are several typical valve-less piezoelectric pumps proposed. Erik Stemme et al invented a valveless diffuser /nozzle-based fluid pump, in which a pair of mutually inverted diffuser /nozzle tubes was fitted at two outsides of the pump chamber[7]. Xia Q X et al proposed a valve-less piezoelectric pump with unsymmetrical slope chamber bottom, in which multi groups of unsymmetrical slope structure were designed in pump chamber[8]. No-moving part valve is one key part of piezoelectric pump. There are various forms of no-moving part valve for valve-less piezoelectric pump, such as tube shaped valves: diffuser/nozzle, Y-shape tube, and special shape tube; different shapes of chamber bottom as valves: flat-cone-shape pump chamber and unsymmetrical slopes element pump chamber; different shapes of bluff-body as valves: multiple rota-table panes inside the pump chamber; bionic valve and so on[9-15]. Both valve-less piezoelectric pumps with tube shaped valve and chamber bottom valve have asymmetric structure at entrance and exit of pump in flow direction by changing the symmetric structure of tubes or surface of chamber bottom. It leads to complex shape and structure of tubes and chamber bottom at entrance and exit of pump, which makes it difficult for machining and structural miniaturization. Consequently the application of these pumps in

Received date: 2021-02-24 **Accepted date:** 2021-03-28

Biographies: Shengduo Li, Master, Associate Professor, research interest: Intelligent control of precision agriculture, Email: lsdhit@163.com; **Wei Zhao,** Postgraduate student, research interests: agriculture aviation technology, Email: 893253225@qq.com; **Xiaoqi Hu**, PhD, Associate Professor, research interest: Microfluidic drive technology, Email: 859002426@qq.com.

*** Corresponding author: Jing Ji,** PhD, Associate Professor, research interest: Microfluidic drives and precision agriculture technology. Mailing Address: College of Mechanical and Electrical Engineering, Qingdao Agricultural University, Qingdao. Email: hcqjijing@163.com. **Caiqi Hu**, PhD, Associate Professor, research interest: Microfluidic drives and precision agriculture technology. Mailing Address: College of Mechanical and Electrical Engineering, Zaozhuang University, Zaozhuang. Email: hucaiqi@163.com.

industry is limited. However, as one type of bluff-body valve, hemisphere-segment has asymmetric surface structure, and works as no-moving part valve when put in the chamber of valve-less piezoelectric pump. The authors have researched and developed this type of valve-less piezoelectric pump with hemisphere-segment bluff-body in preliminary work. Hemisphere-segment can be easily machined, and can work as valve body when it is fitted on the chamber bottom, which leads to different flow resistances at entrance and exit of the pump. This type of valve-less piezoelectric pump has simple inner chamber structure, and the whole structure and processing are also simplified, which meet the needs of micro processing technology.

Valve-less piezoelectric pump with HSBB has good structural machinability, and can be assembled and adjusted conveniently. What's more, this type of pump has great performance on fluid pumping. However, because the valve-less piezoelectric pump with bluff-body is a new type of fluid pump, there is no theoretical research available on its flow resistance property, fluid pumping performance as well as their influencing factors. The fluid pumping performance directly depends on the flow resistance and the change law of flow resistance on HSBB. Moreover, hemisphere-segment has irregular geometrical body shape, and the flow resistance on which relies on its size, shape and orientation. Therefore, the establishment of the resistance formula on hemisphere-segment is far more complex than on sphere, and it is quite difficult to directly research the action law of flow resistance on hemisphere-segment. Whereas, sphere has regular symmetrical shape in space. And the research of flow resistance on sphere has been carried out for a long time, the achievement on which is quite rich [16-20]. The semi-empirical formula and empirical formula of resistance coefficient on sphere have been verified in engineering application. Because hemisphere-segment has some attributes of sphere, obviously it should be an efficient way to analysis hemisphere-segment resistance coefficient with the reference of sphere resistance coefficient calculation method.

By comparing and analyzing it is shown that traditional flow resistance calculation method on non-spherical bluff-body is not suitable for the hemisphere- segment used in the pump proposed in this paper. Comprehensively considering the shape and orientation of hemisphere-segment, the method of Equivalent Flow Resistance Diameter is presented. Based on equivalent flow resistance model, the shapes respectively corresponding to spherical surface and round surface on hemisphere-segment are transformed into two spheres of different diameters. And the equivalent flow resistance diameters on both surfaces of hemisphere-segment are obtained. The experiment device for measuring flow resistance is designed and made. The flow resistance coefficients on different diameter spheres and hemisphere-segment are measured and calculated. Finally, the action law of flow resistance around sphere of different diameter and the coefficient of flow resistance around hemisphere-segment are obtained. By comparing and analyzing the result shows that traditional method is not suitable for hemisphere-segment resistance coefficient calculation. Then the theoretical calculation formulas of flow resistance coefficients on hemisphere-segment in forward and reverse direction are established innovatively, which can be used to analysis and calculate the flow resistance coefficient for valve-less piezoelectric pump with HSBB. Furthermore, the research in this paper can offer reference and direction of the analysis on flow resistance for other valve-less piezoelectric pumps with different geometric shapes bluff-body.

2 Hemisphere-segment and Valve-less Piezoelectric Pump with HSBB

2.1 Geometric and Flow Resistance Characteristic of Hemisphere-segment

The hemisphere-segment is 1/4 sphere obtained from the steel ball at the diameter of φ8 mm by wire cutting. This type of body shape has complex geometry surface features, which are smooth 1/4 spherical surface and vertical 1/2 round surface. Those features make hemisphere-segment having unique flow resistance characteristics. There is schematic of forward and reverse flow-facing surface of hemisphere-segment in Figure 1. If the uniform flow V_1 is defined as forward flow, and V_2 is defined as reverse flow. The flows V_1 and V_2 respectively in the forward and reverse are applied on the spherical surface S_1 and round surface S_2 of the hemisphere-segment. The flow resistance on the smooth spherical surface S_1 is smaller than the one on the vertical round surface S_2; and the flow resistance coefficient C_{D1} on S_1 is also smaller than the flow resistance coefficient C_{D2} on S_2. Consequently, hemisphere-segment can be used as the bluff-body, which can form different flow resistance between forward and reverse flow. Thus the hemisphere-segment bluff-body plays the role of a valve in the valve-less piezoelectric pump chamber and it controls the flow direction of fluid.

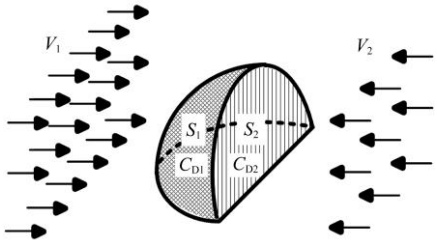

Figure 1 Schematic of forward and reverse flow- facing surface of hemisphere-segment

2.2 Valve-less Piezoelectric Pump with HSBB

The section structure diagram of valve-less piezoelectric pump with HSBB is shown in Figure 2, and the pump chamber is a hollow cylinder. Circular holes P1 and P2 distribute along the circumference of pump chamber and two of them are separated by 180°, hemisphere-segment is mounted at pump base with spherical surface S_1 facing to hole P1 and round surface S_2 facing to hole P2. The periodic vibration of piezoelectric vibrator causes the periodic change of volume and pressure inside pump chamber. When the vibration of piezoelectric vibrator causes the decreasing of pressure inside pump chamber, pump inhales fluid simultaneously from both holes P1 and P2. Because the resistance of fluid flowing around 1/4 spherical surface S_1 is smaller than the one of fluid flowing around 1/2 round surface S_2, the fluid inhaled from hole P1 is more than the one inhaled from hole P2. When the vibration of piezoelectric vibrator causes the increasing of pressure inside pump chamber, pump discharges fluid simultaneously from both holes P1 and P2. Because the resistance of fluid flowing around 1/2 round surface S_2 is bigger than the one of fluid flowing around 1/4 spherical surface S_1, the fluid discharged from hole P2 is more than the one discharged from hole P1, so in one working cycle of the pump, the fluid inhaled from hole P1 is more than the one inhaled from hole P2, the fluid discharged from hole P2 is more than the one discharged from hole P1. Thus at macro level the unidirectional flow of fluid is formed and the performance of

pumping fluid is realized. The pump takes advantage of different shape flow-facing surfaces of hemisphere-segment having different flow resistance, so the flow resistance difference between forward and reverse flow can be formed. Along with Figure 1, it can be shown that the smaller the resistance coefficient of forward flow around hemisphere-segment and the larger the resistance coefficient of reverse flow around hemisphere-segment, the greater the pump flow rate. Thus the resistance property of hemisphere-segment is one of the key factors influencing the performance of pump.

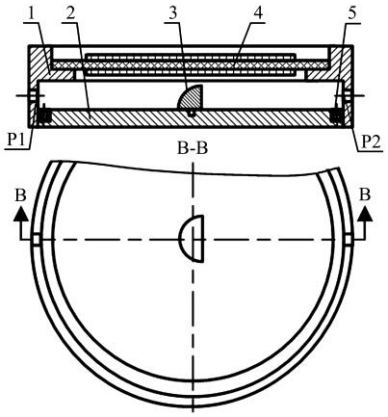

1. Pump chamber 2. Pump base 3. Piezoelectric vibrator 4. Hemisphere-segment 5. O-shape seal ring P1, P2. Circular hole

Figure 2 Structure of valve-less piezoelectric pump with HSBB

2.3 Analysis for Shape Factors of Hemisphere- segment

Shape factor is the parameter that describes the similarity degree of irregular objects approximated to its similar-shape objects. Because hemisphere-segment is part of a sphere, its shape property can be defined as sphericity φ[21]. Sphericity refers to the similarity degree of non-spherical objects approximated to spherical objects. And sphericity φ is calculated by the ratio of the surface area A_b of spherical object and the actual surface area A_p of non-spherical object, and here the spherical object and the non-spherical object have equal volume. V_p and A_p are defined respectively as the volume and the surface area of hemisphere-segment, and the sphericity φ of hemisphere-segment can be expressed as follows:

$$\varphi = \frac{A_b}{A_p} = \frac{(36\pi V_P^2)^{\frac{1}{3}}}{A_P} = 0.7938 \quad (1)$$

The sphericity of sphere is φ=1. According to formula (1), it can be concluded that hemisphere-segment is close to sphere.

Because of hemisphere-segment inherent irregular geometrical shape obviously it can be very difficult to study directly the action law of flow resistance around hemisphere-segment. However the spatial symmetric structure and equal flow resistance at arbitrary orientation of sphere, its flow resistance coefficient expression can be obtained easily. According to the conclusion above that the sphericity of hemisphere-segment is close to that of sphere, the flow resistance coefficient calculation of sphere can be used to approximately calculate the flow resistance coefficient of hemisphere-segment.

3 Traditional Non-spheroid Equivalent Sphere Diameter Method Applied to HSBB in Pump

Presently there are two main kinds of research about the resistance around non-spherical bluff-body. One is the research of flow resistance around ellipsoid[22], cylinder[23], disc[24] and et al., which have definite shape and orientation. In this kind of research, for corresponding shape a good calculation result can be obtained, but it cannot be used for the resistance analysis on bluff-body of other shapes and orientations. In the other method non-spheroid is transformed into sphere by Equivalent Volume Diameter[21], and the transformed sphere has equal volume with the non-spheroid. Then the resistance coefficient of non-spheroid can be calculated and properly modified through sphere resistance expression.

Among the two methods above the second one is more universal for the flow resistance coefficient calculation of non-spheroid. But with the second method for a definite hemisphere-segment there is only one diameter of sphere after equivalently transformed. Namely the hemisphere-segment is equivalent to one sphere after transformation. And we know that the flow resistance coefficients of sphere in any direction along the circumference are equal. It means that the forward and reverse flow resistances on hemisphere-segment are equal after equivalently transformed, which is contrary to the different flow resistances in forward and reverse flow-facing surface of hemisphere-segment shown in Figure 1. Obviously the traditional method of Equivalent Volume Diameter above is not suitable for the flow resistance analysis of hemisphere-segment bluff-body in pump.

The main reason is that the traditional equivalent diameter method by transforming non-spherical bluff-body into similar sphere is only effective for the flow resistance analysis of bluff-body with single orientation. As for hemisphere-segment in pump, the resistances of spherical surface and round surface to fluid are different. The traditional method of Equivalent Volume Diameter transforms both of spherical surface and round surface into spherical surface. The transformed body lost hemisphere-segment inherent geometrical features. Thus it lost the features of hemisphere-segment valve. Hemisphere-segment valve proposed in this paper precisely utilizes the different flow orientations on the two different flow-facing surfaces of hemisphere-segment to form the flow resistance difference. So the traditional equivalent diameter method is not suitable for the transformation of HSBB into similar spherical model.

4 Separation of Forward and Reverse Flow Equivalent Sphere Diameters for Hemisphere-segment Based on Equivalent Flow Resistance

4.1 Equivalent Flow Resistance Diameter Model

In order to analyze the forward and reverse flow resistance property of hemisphere-segment based on flow resistance distribution law of sphere, the hemisphere-segment should be transformed into equivalent similar-sphere model. Since traditional equivalent volume diameter method is not suitable for hemisphere-segment model, in this paper the equivalent flow resistance diameter method is innovatively proposed. According to the requirements of the flow-facing and flow-dorsal surfaces of hemisphere-segment on definite flow orientations, hemisphere-segments respectively for the flow-facing and flow-dorsal surfaces are transformed into equivalent flow resistance sphere model. Essentially it means that the sphere diameters are researched, in other words the diameters of the spheres are analyzed and calculated. As shown in Figure 3, forward and reverse uniform flows are applied on the spherical surface S_1 and round surface S_2 respectively at the flow velocity of V_1 and V_2. The flow resistance on fluid caused by spherical

surface S_1 is equivalent to that caused by the sphere at the diameter of d_1. And the flow resistance caused by round surface S_2 is equivalent to that caused by the sphere at the diameter of d_2. Namely, diameters d_1 and d_2 are the equivalent flow resistance sphere diameters on forward and reverse flow of hemisphere-segment. In order to obtain the specific values of equivalent flow resistance diameter d_1 and d_2, the experiment is designed and carried out through measuring the flow resistances of multiple different diameter spheres and hemisphere-segment as follows.

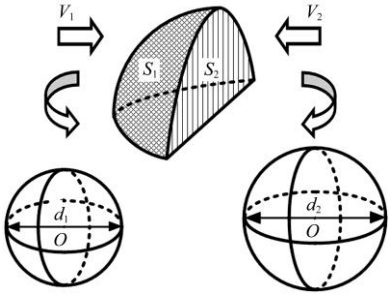

Figure 3 Schematic of equivalent flow resistance diameter for hemisphere-segment

4.2 Flow Resistance Measuring Device

In order to determine the flow resistance coefficients of hemisphere-segment and different diameter spheres, the experimental device is designed as shown in Figure 4. It can automatically or semi- automatically fills water to the working tank and keeps the stable water level in the working tank[23]. The experimental device consists of water storage tank, working tank, floater part, piezoelectric pump with HSBB, measuring graduate and electronic balance (measuring accuracy is 0.1 g), and so on. H is the height distance from the constant water level in the working tank to the horizontal center plane of the pump chamber.

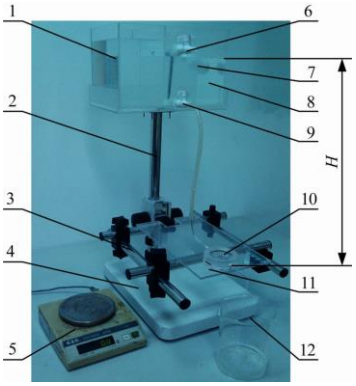

1. Water storage tank 2. Screw stem 3. Stand 4. Base 5. Electronic balance 6. Relief valve 7. Floater part 8. Working tank 9. One-way valve 10. Prototype pump 11. Loading plate 12. Measuring cup

Figure. 4 Measuring device for flow resistance on hemisphere-segment

Water is chosen as the measuring fluid. In addition, floater part is used to feed water so as to keep the definite level of water in the working tank during the experiment. What's more, there is a relief valve on the working tank. When the water level in the working tank is higher than the set position, the superfluous fluid can be drained out through relief valve.

Based on the Bernoulli's Energy Equation and Energy Conservation Equation, the flow resistance coefficients are obtained by calculating the kinetic energy loss of water when it flows respectively through hemisphere-segment and spheres. The flow resistance coefficient experimental formula is shown as Eqs. (2)-(3) (the derivation process is discussed in another paper).

$$C_D = \frac{v_0^2 - v_1^2}{v_1^2} \tag{2}$$

$$Q = Avt \tag{3}$$

where, v_0 and v_1 respectively are the average flow velocities in pump chamber without and with sphere or hemisphere-segment; C_D is the flow resistance coefficient; Q is the flow quantity in t time; A is the section area through the center of pump chamber; the average flow velocities v_0 and v_1 in equation (2) are obtained from equation (3) and v refers to v_0 or v_1.

By the experiment the time t of the specific quantity water Q draining out from pump chamber is measured under the conditions: 1) with sphere in pump chamber; 2) without sphere or hemisphere-segment in pump chamber; 3) with hemisphere-segment in pump chamber. Then those values of t and Q are substituted into Eqs. (2)-(3), and the flow resistance coefficients C_D of spheres and hemisphere-segment can be calculated.

4.3 Flow Resistance Measuring and Calculating for Different Diameter Spheres

Different diameter spheres(φ3.5 mm, φ4.0 mm, φ4.5 mm, φ5.0 mm, φ5.5 mm, φ6.0 mm, φ6.35 mm, φ7 mm) are used in the experiment. The material of all spheres is stainless steel. Based on the experiment device (shown in Figure 4) the flow resistances of all spheres are measured at the same time in the same environment.

In order to measure the flow resistance coefficients of spheres with different diameters, the height distance from the constant water level in the working tank to the horizontal center plane of the pump chamber is set as H=300 mm. The time needed to discharge the fixed flow quantity water of Q=300 mL from the pump chamber without spheres is defined as t_0. The time needed to discharge the fixed flow quantity water of Q=300 mL from the pump chamber with spheres is defined as t_1. The times t_0 and t_1 are measured. Then the flow velocities and resistance coefficients can be obtained based on resistance coefficient computational equation (2) and flow quantity equation (3). The relationship between the flow resistance coefficients C_D of spheres in the diameters of φ3.5 mm~φ7 mm and the sphere diameters d is shown in Figure 5.

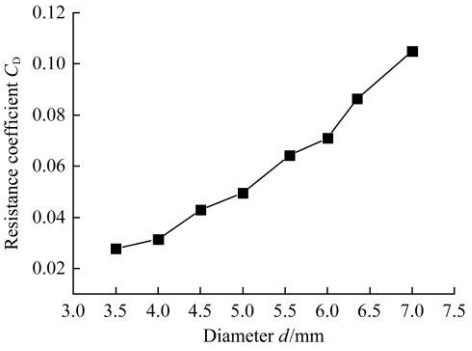

Figure 5 Relation curve of resistance coefficient and diameter of sphere

From Figure 5 it can be shown that the flow resistance coefficient of sphere increases along with the increase of sphere diameter. It means that the flow-facing surface area of sphere increases along with sphere diameter increasing, which leads to the increasing of frictional resistance.

Based on the experimental data of the resistance coefficient of different diameter spheres, the resistance coefficient expression of different diameter spheres is obtained by nonlinear regression and

is shown as follows.

$$C_D = 0.003d^2 - 0.014d + 0.033 \quad (4)$$

4.4 Measuring for Forward and Reverse Flow Resistance of Hemisphere-segment

In order to obtain the forward and reverse flow resistance coefficient of hemisphere-segment, the height H is set as H=100-700 mm. The time needed to discharge the water of Q=300 mL from the pump chamber without hemisphere-segment is defined as t_0 and the flow velocity is defined as v_0. The time needed to discharge the water of Q=300 mL from the pump chamber with hemisphere-segment in forward position is defined as t_1 and the flow velocity is defined as v_1. The time needed to discharge the water of Q=300 mL from the pump chamber with hemisphere-segment in reverse position is defined as t_2 and the flow velocity is defined as v_2. The times t_0, t_1 and t_2 are measured. Then the flow velocities v_0, v_1, and v_2, the forward flow resistance coefficient C_{D1} and the reverse flow resistance coefficient C_{D2} can be obtained based on resistance coefficient equation (2) and flow quantity equation (3). The experimental and computational data of flow resistance on hemisphere-segment are shown in Table 1.

Table 1 Experimental and computational data of flow resistance around hemisphere-segment

H/mm	t_0/s	t_1/s	C_{D1}	t_2/s	C_{D2}	v_1/m·s^{-1}	v_2/m·s^{-1}	v_0/m·s^{-1}
100	117.10	121.00	0.065634	122.50	0.092218	0.236851	0.233951	0.2445
150	87.85	90.50	0.059167	91.50	0.082704	0.316674	0.313213	0.325908
200	71.10	73.10	0.054986	74.00	0.081123	0.392052	0.387284	0.402686
250	61.60	63.25	0.05223	64.00	0.077332	0.453107	0.447797	0.464789
300	56.00	57.35	0.04675	58.07	0.07319	0.49972	0.49353	0.51127
350	51.60	52.75	0.043029	53.40	0.068893	0.543299	0.536685	0.554864
400	42.23	43.10	0.039593	43.55	0.061415	0.664942	0.658071	0.677978
600	37.75	38.50	0.038098	38.90	0.059781	0.74439	0.736735	0.758437
700	35.75	36.43	0.036376	36.80	0.057534	0.786687	0.778777	0.800867

4.5 Calculating Forward and Reverse Equivalent Sphere Diameters of Hemisphere-segment Based on Equivalent Flow Resistance

According to the data in Table 1 and the method of Equivalent Flow Resistance, forward and reverse equivalent sphere diameters of hemisphere-segment are calculated. From Table1 at the height of H=300 mm, the forward and reverse resistance coefficients of hemisphere-segment respectively are C_{D1}=0.04675 and C_{D2}=0.07319, the two values of C_{D1} and C_{D2} are respectively substituted into equation (4), which means that at the same height condition the forward and reverse resistance coefficient values of hemisphere-segment are respectively equal to the resistance coefficient values of different diameter spheres. And the following equations can be obtained:

$$C_{D1} = 0.04675 = 0.003d_1^2 - 0.014d_1 + 0.033 \quad (5)$$

$$C_{D2} = 0.07319 = 0.003d_2^2 - 0.014d_2 + 0.033 \quad (6)$$

Eqs. (5)-(6) are solved to obtain d_1=5.50 mm, d_2=6.67 mm, which means that the forward and reverse equivalent sphere diameters of hemisphere-segment respectively are φ5.50 mm and φ6.67 mm according to the method of equivalent flow resistance.

According to forward and reverse equivalent sphere diameters d_1 and d_2 of hemisphere-segment, forward and reverse equivalent Reynolds numbers Re_1 and Re_2 can be calculated. Hence, the relation curve of Reynolds number and resistance coefficient of hemisphere-segment can be obtained shown in Figure 6 (Re_p, p=1, 2).

As shown in Figure 6 for hemisphere-segment with given diameter, its forward and reverse flow resistance coefficient decrease along with the increase of Re_p, which is consistent with the changing trend of classical sphere flow resistance coefficient in the reference [26]. As Re_p changes, forward flow resistance coefficient C_{D1} is far less than reverse flow resistance coefficient C_{D2}, which is consistent with the conclusion that the flow resistance around smooth surface is less than the flow resistance around vertical surface in flow theory analysis. The two conclusions above verify that the experimental conditions and environment proposed in this paper are feasible and reasonable. What's more, as Re_p changes, the changing range of the resistance coefficient difference between in forward and reverse is stable. In other words the resistance coefficient difference tends to a stable value in a wide range of Re_p, which provides the theoretical support for the research in this paper that the stable pumping flow can be formed in valve-less piezoelectric pump with HSBB.

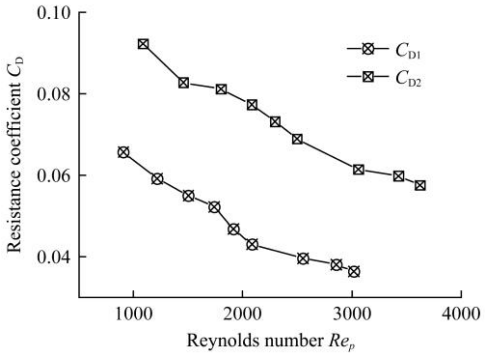

Figure 6 Relation curve of forward, reverse resistance coefficient and Reynolds number of hemisphere-segment

Synthesizing the analysis above, so far the transformation of hemisphere-segment into equivalent sphere by Equivalent Flow Resistance has been realized. Then the flow resistance coefficient of hemisphere-segment will be calculated by the flow resistance coefficient equation of sphere as the following.

5 Analysis of Flow Resistance Coefficient Correlation Equation of Hemisphere-segment by Traditional Method

There are some researches on flow resistance around sphere for a long time[17,26]. Among them, the flow resistance coefficient equation presented by Clift and Gauvin through experimental data fitted in 1978 is the best one, and has been widely used. Clift&Gauvin equation is as follows[26].

$$C_D = \frac{24}{Re}(1 + 0.15Re^{0.687}) + \frac{0.42}{1 + 4.25 \times 10^4 Re^{-1.16}} \quad (7)$$

$$Re = \frac{Vd}{\nu}$$

where, V is flow velocity of fluid; v is kinematic viscosity of fluid; d is sphere diameter.

The Reynolds numbers of flow around hemisphere-segment can be defined by its equivalent flow resistance diameter d_1 and d_2. And then the equivalent Reynolds number Re_1 and Re_2 of forward and reverse flow around hemisphere-segment can be obtained. Hence, the Clift correlation equation of forward and reverse flow resistance coefficient C_{D1L}, C_{D2L} of hemisphere-segment is shown as follows:

$$C_{D1L} = \frac{24}{Re_1}(1+0.15Re_1^{0.687}) + \frac{0.42}{1+4.25\times10^4 Re_1^{-1.16}} \tag{8}$$

$$C_{D2L} = \frac{24}{Re_2}(1+0.15Re_2^{0.687}) + \frac{0.42}{1+4.25\times10^4 Re_2^{-1.16}} \tag{9}$$

As shown in Table 2 there are comparisons between theoretical values (by Eqs. (8)-(9)) and experimental values (obtained from Table 1). Within experimental Reynolds number range, the theoretical value has the same changing trend with experimental value. Both of theoretical and experimental value decrease along with the increase of *Re*. But there are very large relative deviations between theoretical and experimental value respectively in forward and reverse flow. The average relative deviation in forward flow is 774% and the average relative deviation in reverse flow is 465%.

Table 2 Comparison for theoretical and experimental values of forward, reverse resistance coefficient

H/mm	Re_1	Forward		Re_2	Reverse	
		C_{D1L}	C_{D1}		C_{D2L}	C_{D2}
100	908	0.4561	0.0656	1088	0.4561	0.0922
150	1214	0.4439	0.0592	1456	0.4263	0.0827
200	1503	0.4236	0.0550	1801	0.4097	0.0811
250	1737	0.4122	0.0522	2082	0.4007	0.0773
300	1916	0.4056	0.0467	2295	0.3958	0.0732
350	2083	0.4007	0.0430	2496	0.3923	0.0689
400	2550	0.3915	0.0396	3060	0.3864	0.0614
600	2855	0.3880	0.0381	3426	0.3848	0.0598
700	3017	0.3867	0.0364	3622	0.3844	0.0575

where, R_{e1} is forward Reynolds number; R_{e2} is reverse Reynolds number; C_{D1L}, C_{D1} are respectively theoretical and experimental values of forward flow resistance coefficient; C_{D2L}, C_{D2} are respectively theoretical and experimental values of reverse flow resistance coefficient; C_{D1}, C_{D2} are obtained from Table 1.

According to the comparison and analysis above, it can be seen that although the change trends of traditional theoretical value (obtained by Clift correlation equation) and experimental value are respectively consistent in two directions, but there are very large deviations between traditional theoretical and experimental value. However it is difficult to obtain high precision through modification. The conclusion can be obtained that it is not feasible to calculate hemisphere-segment resistance coefficient by above method of the analogy sphere resistance coefficient. So innovative method are needed to solve the flow resistance coefficient of hemisphere-segment.

6 Formula Derivation and Experimental Verification of Hemisphere-segment Flow Resistance Coefficient by Innovative Method

6.1 Formula Derivation of Flow Resistance Coefficient for Hemisphere-segment

According to above analysis, the area S_1 is the flow-facing surface area of 1/4 spherical surface and S_2 is the flow-facing surface area of 1/2 round surface (shown in Figure 2). Re_1 and Re_2 are respectively the Reynolds numbers defined by equivalent flow resistance diameter d_1 and d_2. Based on the above flow resistance theoretical analysis, the forward and reverse resistance coefficient experimental results of hemisphere-segment and different diameter spheres, it can be concluded that spherical flow-facing surface S_1 has less resistance on fluid than round flow-facing surface S_2 does. And with the increase of spherical surface area S_1 and round surface area S_2, both of their resistance on fluid change in a proportional trend. Moreover, the action law of equivalent Reynolds number Re_1 and Re_2 of hemisphere-segment on flow resistance is consistent with the action law of sphere does. That is, with Re_1 and Re_2 increasing, the flow resistances vary according to the power index law. Hence, the relations between the forward and reverse flow resistance coefficients C_{D1}, C_{D2} and the flow-facing surface areas S_1, S_2 and the Reynolds numbers Re_1, Re_2 for hemisphere-segment are given as Eqs. (10)-(11).

$$C_{D1} = a\times S_1 \times Re_1^b \tag{10}$$

$$C_{D2} = c\times S_2 \times Re_2^d \tag{11}$$

where a, b, c and d are undetermined parameters.

Based on the forward and reverse resistance coefficients (in Table 1) and their corresponding Reynolds numbers (in Figure 6), the parameters of forward and reverse flow resistance coefficient can be obtained by fitting operation: $a = 0.0389$, $b = -0.494$, $c = 0.0538$ and $d = -0.381$. Then the values of a, b, c and d are substituted into Eqs. (10)-(11), and the expressions can be gotten as Eqs. (12)-(13):

$$C_{D1} = a\times S_1 \times Re_1^b = 1.955Re_1^{-0.494} = \frac{1.955}{Re_1^{0.494}} \tag{12}$$

$$C_{D2} = c\times S_2 \times Re_2^d = 1.351Re_2^{-0.381} = \frac{1.351}{Re_2^{0.381}} \tag{13}$$

Eqs. (12)-(13) are theoretical derivation formulas of forward and reverse flow resistance coefficient for hemisphere-segment.

6.2 Experimental Verification

In order to verify the fluid pumping effect of valve-less piezoelectric pump with HSBB and the above theoretical analysis, the comparison between theoretical and experimental pumping flow rate is carried out.

The theoretical pumping flow rate Q_L formula of valve-less piezoelectric pump with HSBB refers to shown as the following[18]:

$$Q_L = f\Delta V(\varsigma_1 - \varsigma_2)/2(1-\varsigma_1\varsigma_2) \tag{14}$$

$$\varsigma_1 = \left(1-a(1+C_{D1})\right)^{1/2} \Big/ \left(1-a+C_{D1}\right)^{1/2}$$

$$\varsigma_2 = (1-a+C_{D2})^{1/2} \Big/ \left(1-a(1+C_{D2})\right)^{1/2}$$

$$a = A_0^2/A^2$$

where, f — vibration frequency of piezoelectric vibrator; A_0 — cross-sectional area of inlet or outlet pipe; A—sectional area of pump chamber through its center; C_{D1}—forward flow resistance coefficient of hemisphere-segment; C_{D2}—reverse flow resistance coefficient of hemisphere-segment; ΔV—variable quantity of pump chamber volume when piezoelectric vibrator working.

Eqs. (12)-(14) are jointly solved, and the theoretical pumping flow rate Q_L can be obtained at f=2-6 Hz, which is shown in Figure 8.

The experimental pumping flow rate is measured as shown in Figure 7. Signal generator and low frequency power amplifier provide the driving voltage and vibration frequency of piezoelectric vibrator. Water is chosen as fluid medium for the experiment. A

hemisphere-segment of diameter = φ8 mm is fixed in the chamber of prototype pump. One end of the inlet pipe faces directly on 1/4 spherical surface of the hemisphere-segment, the other end of the inlet pipe is inserted into water storage measuring glass, which is filled with water in advance and continuously injected with water by water pipe in experiment process so as to guarantee the stability of water level in the water storage measuring glass. At the driving voltage U = 120v and frequency f = 2-6 Hz the experimental pumping flow rate Q_S is shown in Figure 8.

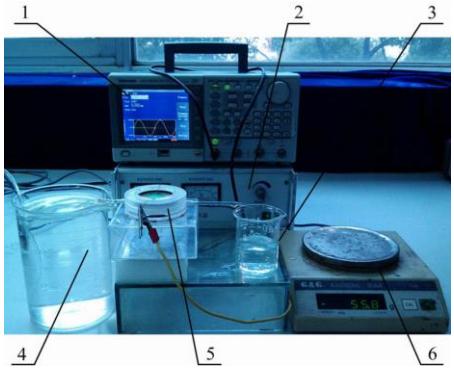

1. Signal generator 2. Low frequency power amplifier 3. Small measuring cup 4. Sater storage measuring cup 5. Prototype pump 6. Electronic balance

Figure 7 Pump flow rate experiment

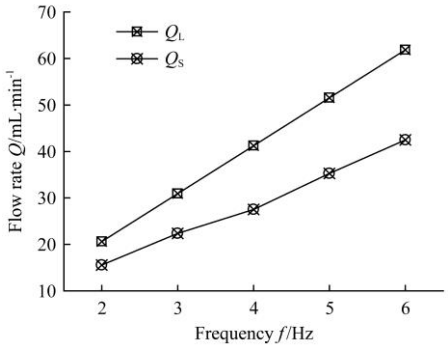

Note: Q_L— the theoretical pumping flow rate; Q_S— the experimental pumping flow rate.

Figure 8 Comparison between experimental and theoretical pumping flow rate

As shown in Figure 8, experimental and theoretical pumping flow rate vary in a consistent trend in a definite frequency range. The minimum relative deviation of them is 24.75%, and the maximum relative deviation of them is 31.15%. And it is feasible that the flow resistance and flow quantity are analyzed and approximately calculated by the forward and reverse flow resistance coefficient formulas of hemisphere-segment innovatively proposed in this paper. But there is still large deviation between experimental and theoretical flow rate, the main reason of which is that in an actual flow field there are some collisions between the vortexes, and these collisions cause the consumption of kinetic energy, however it is ignored in the theoretical flow rate calculation.

7 Conclusions

(1) The important problem is found that the forward and reverse flow resistances on HSBB can not be solved simultaneously by traditional theoretical and experimental hydrodynamics equivalent method for flow resistance around non-sphere, and the essential reason is revealed. The method of Equivalent Flow Resistance Diameter is presented and used to research the flow resistance law of hemisphere-segment.

(2) The forward and reverse flow-facing surfaces of hemisphere-segment respectively corresponding to spherical and round surfaces are transformed into spheres with the diameter d_1 and d_2 according to equivalent sphere model. The flow resistance experiment device is designed and fabricated. The flow resistance is measured by the device. Combined with theoretical analysis the forward and reverse equivalent flow resistance diameters of hemisphere-segment are derived.

(3) The change law of flow resistance coefficients for flowing around hemisphere-segment is obtained. And it is verified that the law can be applied to analyze and calculate the flow resistance and flow rate of pump.

The research in this paper shows that the method of Equivalent Flow Resistance Diameter and flow resistance coefficient theoretical formulas of hemisphere-segment provide new ideas for flow resistance property analysis of hemisphere-segment in valve-less piezoelectric pump. What's more, the theoretical basis is established for the further research on flow resistance property of multiple hemisphere-segments in different layouts. And the reference and guidance effects are provided for flow resistance analysis of valve-less piezoelectric pump with other geometrical bluff-body.

The hemisphere-segment is one simple no-moving part valve of all the bluff-bodies. In the actual application of mixing and pumping fluid, the bluff-body valves with different structures can be optimized and composed, and the flow resistance difference can be enlarged, then the flow rate range can be enlarge, and the mixing and pumping effect can be improved , so that the valve-less pump can exert its advantages in precision agricultural plant protection spraying.

Acknowledgments

We deeply thank for National Natural Science Foundation of China (Grant No. 31971801), Natural Science Foundation of Shandong Province (No. ZR2020ME250, No. ZR2020ME252).

[References]

[1] Lintel V H T G, Pol V D F C, Bouwstra S. A piezoelectric micropump based on micromachining of silicon. Sensors and Actuators, 1988, 15(2): 153–167.

[2] Shoji S, Nakagawa S, Esashi M. Micropump and sample-injector for integrated chemical analyzing systems. Sensors and Actuators A: Physical, 1990, 21(1-3): 189–192.

[3] Ederer I, Raetsch P, Chullerus W S, et al. Piezoelectric driven micropump for on-demand fuel-drop generation in an automobile heater with continuously adjustable power output. Sensors and Actuators A: Physical, 1997, 62(1-3): 752–755.

[4] Yan X J, Yuan H Z, Zhou X X, et al. Control efficacy of different pesticide formulations and fan-nozzle model on wheat aphids by UAVs. Int J Precis Agric Aviat, 2020, 3(2): 35–39.

[5] Zhou Q Q, Xue X Y, Qin W C, et al. Analysis of pesticide use efficiency of a UAV sprayer at different growth stages of rice. Int J Precis Agric Aviat, 2020, 3(1): 38–42.

[6] Kong H, Yi L L, Lan Y B, et al. Exploring the operation mode of spraying cotton defoliation agent by plant protection UAV. Int J Precis Agric Aviat, 2020, 3(1): 43–48.

[7] Erik S, Goran S. A valve-less diffuser /nozzle-based fluid pump. Sensors and Actuators A, 1993, 39(12): 159–167.

[8] Xia Q X, Zhang J H, Lei H, et al. Theoretical Analysis and Experimental Verification on Flow Field of Piezoelectric Pump with Unsymmetrical Slopes Element. Chinese Journal of Mechanical Engineering, 2009, 22(5): 735–744. (in Chinese)

[9] Zhang J H, Li Y L, Xia Q X. Analysis of the pump volume flow rate and tube property of the piezoelectric valve-less pump with Y-shape tubes. Chinese Journal of Mechanical Engineering, 2007, 43(11): 136–141. (in Chinese)

[10] Huang J, Zhang J H, Wang S Y. Theory and experimental verification on valve-less piezoelectric pump with multistage Y-shape tubes. Opt. Precision Eng., 2013, 21(2): 423–430. (in Chinese)
[11] Izzo I, Accoto D, Menciassi A, et al. Modeling and experimental validation of a piezoelectric micropump with novel no-moving-part valves. Sensors and Actuators A: Physical, 2007, 133(1): 128–140.
[12] Forster F K, Williams B E. Parametric design of fixed-geometry microvalves—the Tesser valve. Proceedings IMECE, Paper, 2002 (33628): 431–437.
[13] Forster F K, Walter T. Design Optimization of Fixed-Valve Micropumps for Miniature Cooling Systems. ASME Conference Proceedings, 2007(42770): 137–145.
[14] Wu L P. Theoretical and experimental research of valve-less piezoelectric pump with Flat-cone-shape pump chamber. Changchun: Jilin University, 2008. (in Chinese)
[15] Zhang J H, Li H, Zhao C S. The Valve-less Piezoelectric Pump with Multiple Rotatable Panes inside: China ZL 22006 1 0114526.8. http://pdf.soopat.com/TiffFile/PdfView/35158FB600C93EDA6F0DC588B53988D6. (in Chinese)
[16] Wu W Y. Fluid Mechanics. Beijing: Peking University Press, 1983. (in Chinese)
[17] Lin J Zh. Fluid-solid two-phase coherent vortex flow and hydrodynamic stability. Beijing: Tsinghua University Press, 2003. (in Chinese)
[18] Ge Z T, Ji J, Lan Y B, et al. Analysis and test on influence of caudal- fin on performance of valveless piezoelectric pump. Journal of Drainage and Irrigation Machinery Engineering, 2017,35(01): 87–92.
[19] Fu J, Zhang J H, Wang Y, et al. Research on semi-flexible valve piezoelectric pump. Journal of Vibration Measurement & Diagnosis, 2019, 39(05): 1005–1010.
[20] Ji J, Zhang J H, Xia Q X, et al. Theoretical Analysis and Experimental Verification on Valve-less Piezoelectric Pump with Hemisphere-segment Bluff-body. Chinese Journal of Mechanical Engineering, 2014, 27(3): 595–605. (in Chinese)
[21] Zheng S L, Yuan J Z. Machining technique and application manual of non-metallic mines. Beijing: Metallurgical Industry Press, 2005. (in Chinese).
[22] Tripathi A, Chhabra R P, Sundararajan T. Predictions of drag and shape of a fluid particle in creeping flow by upper bound approach. International Journal of Engineering Science, 1995, 33(1): 13–25.
[23] Ui T J, Husseyr R G, Roger R P. Stokes drag on a cylinder in axial motion Physics of Fluids, 1984, 27(4): 787–795.
[24] Davis A M J. Stokes drag on a disk sedimenting toward a plane or with other disks: additional effects of a side wall or free surface. Physics of Fluids A: Fluid Dynamics, 1990, **2**(3): 301–312.
[25] Ji J, Zhang J H, Zhao C. Flow resistance measuring device for valve-less piezoelectric pump: China, 201310243970.X. 2013. (in Chinese)
[26] Clift R, Grace J R, Weber M E. Bubbles, Drops and Particles. New York: Academic Press, 1978.